Imaginary potential for exotic nuclei

G. Pollarolo
Dipartimento di Fisca Teorica, Universitá di Torino and INFN Sezione di Torino, Via Pietro Giuria 1, 10125 Torino, Italy

L. S. Ferreira
Centro de Física das Interacções Fundamentais, Instituto Superior Técnico, Avenida Rovisco Pais, P-1096 Lisbon Codex, Portugal

R. J. Liotta
Royal Institute of Technology, Physics at Frescati, S-10405 Stockholm, Sweden

E. Maglione
Dipartimento di Fisica ''Galileo Galilei,'' Via Marzolo 8, I-35131 Padova, Italy
and INFN, Padova, Italy

(Received 22 September 1998)

The imaginary and polarization potential for reactions involving exotic nuclei is calculated in terms of one-particle transfer channels. Special attention is devoted to transitions to the continuum since for exotic nuclei the Fermi energy is very close to the continuum threshold. [S0556-2813(99)01903-2]

PACS number(s): 24.10.Ht

I. INTRODUCTION

The optical potential is widely used in the analysis of elastic scattering data among heavy ions. In this approximation, the coupling of the elastic channel to the reaction channels is taken into account partly through an imaginary part iW, which takes into account the depopulation of the entrance channel, and partly through a modification of the real part of the potential (polarization). Since the population of the exit channels depends on the bombarding energy these two terms have an intrinsic energy dependence.

The optical potential is not only used to describe elastic scattering data but also to extract nuclear structure information from grazing reactions, usually through distorted wave Born approximation (DWBA) calculations. This will be also the case for exotic nuclei and thus it is quite important to know how the optical potential changes while one approaches the drip lines.

In this paper we will study the imaginary part of the optical potential and the correction to the corresponding real part (polarization term) due to transfer channels in reactions involving exotic nuclei. The effect of the transfer channels will be included by using the semiclassical model of Ref. [1]. This proved to be quite successful for stable nuclei [2]. For exotic nuclei the Fermi level is close to (or even immersed in) the continuum and therefore we have to extend that semiclassical approach to incorporate transitions also to the continuum. In Sec. II we will briefly summarize the most important results of Refs. [1–3], in Sec. III we will discuss the transitions to the continuum, and in Sec. IV numerical applications corresponding to reactions of calcium isotopes on ^{124}Sn target are presented.

II. SEMICLASSICAL THEORY FOR ABSORPTION AND POLARIZATION

In this section we will briefly summarize the formalism of Refs. [1–3]. For convenience of presentation we will only consider the case of angular momentum transfer $\lambda=0$, since the generalization to other cases is straightforward.

The potential that is most commonly used in the optical model analysis of elastic scattering is of the general form

$$U=V+\Delta U=V+\Delta V+iW, \tag{1}$$

where W is the absorptive potential and ΔV the polarization potential that corrects the bare real potential V. The elastic scattering amplitude can be written in general as

$$f_{\alpha\alpha}=\frac{i}{2\kappa}\sum_l\ (2l-1)P_l(\cos\theta)(1-e^{-2i\beta_l}a^l_{\alpha\alpha}) \tag{2}$$

where β_l is the real phase shift due to the bare real potential V and $a^l_{\alpha\alpha}$ is the reaction amplitude for the elastic channel. Up to second order in semiclassical perturbation theory this amplitude may be written in the form

$$a^l_{\alpha\alpha}=1-\frac{1}{\hbar^2}\sum_\gamma\ \int_{-\infty}^{+\infty}dtV_{\alpha\gamma}[r(t)]e^{-i\omega_\gamma t}\times\int_{-\infty}^{t}dt'V_{\gamma\alpha}[r(t')]e^{i\omega_\gamma t'}, \tag{3}$$

where $V_{\alpha\gamma}$ specifies the form factor that couples the entrance channel α $(E_\alpha=0)$ with the intermediate channel γ at an energy $E_\gamma=\hbar\omega_\gamma$. The integration over time is carried out along the classical trajectory corresponding to the impact parameter $\rho=l/\kappa$, where κ is the asymptotic wave number in the entrance channel, i.e., with standard notation $\kappa=(2\mu E/\hbar^2)^{1/2}$.

In the optical model approximation the effect of the coupling is taken into account by modifying the potential V by an amount ΔU such that the phase shift $\tilde{\beta}_l$, calculated with the new potential, satisfy the relation

 ©1999 The American Physical Society

$$e^{2i\tilde{\beta}_l}=e^{2i\beta_l}a_{\alpha\alpha}. \tag{4}$$

In the spirit of the semiclassical approximation one can write

$$e^{2i\tilde{\beta}_l}=e^{2i\beta_l}\left\{1-\frac{i}{\hbar}\int_{-\infty}^{+\infty}dt\Delta U\right\} \tag{5}$$

and thus, from a simple comparison between the above relations, one obtains

$$\int_{-\infty}^{+\infty}dt\Delta U=-\frac{i}{\hbar}\sum_{\gamma}\int_{-\infty}^{+\infty}dtV_{\alpha\gamma}[r(t)]e^{-i\omega_\gamma t}\times\int_{-\infty}^{t}dt'V_{\gamma\alpha}[r(t')]e^{i\omega_\gamma t'}. \tag{6}$$

As it stands, this equation defines for each partial wave l the value that should have the integral of ΔU but not the function $\Delta U(r)$ itself. In order to evaluate this we exploit the fact that in the surface region the form factors are of the form $V_{\alpha\gamma}(r)\sim e^{-r/a_\gamma}$ and that the main contribution to the integral is coming from distances close to the classical turning point r_0. Using for the trajectory its parabolic approximation

$$r=r_0+\frac{1}{2}\ddot{r}_0t^2, \tag{7}$$

where $\ddot{r}_0$ is the radial acceleration at the distance of closest approach, one gets (for more details see Refs. [1,3])

$$\Delta U=-\frac{i}{\hbar}\sum_{\gamma}|V_{\alpha\gamma}(r)|^2\sqrt{\frac{\ddot{r}_0}{\pi a_\gamma}}I(\omega_\gamma), \tag{8}$$

where

$$I(\omega_\gamma)=\int_{-\infty}^{+\infty}dt\,\exp\left(-\frac{\ddot{r}_0}{2a_\gamma}t^2-i\omega_\gamma t\right)\times\int_{-\infty}^{t}dt'\,\exp\left(-\frac{\ddot{r}_0}{2a_\gamma}t'^2+i\omega_\gamma t'\right) \tag{9}$$

is the function that weights the contribution of the different reaction channels to the imaginary and polarization parts of the optical potential.

One-particle transfer channels are dominant to build up the imaginary part of the optical potential in the surface region [2]. In the case of stripping reactions $a+A\rightarrow b+B$, where $a\equiv b+1$ and $B\equiv A+1$, the form factor requires the evaluation of integrals of the form

$$f_{a_2a_1}(\mathbf{r})=\int d^3r_{1A}\phi^{a_2}(\mathbf{r}_{1A})^*U_{1A}(r_{1A})\phi^{a_1}(\mathbf{r}_{1b}), \tag{10}$$

where ϕ^{a_1} and ϕ^{a_2} are the single particle wave functions in the projectile and target, respectively, and $U_{1A}(r_{1A})$ is the shell model potential binding the transferred nucleon to the nucleus A. The label a_1 indicates the quantum numbers (n_1,l_1,j_1,m_1) in the projectile a while a_2 indicates the levels of the targetlike B.

Up to this point we have not included any angular momentum in the formalism. This can be done expanding the form factor given above in spherical waves carrying angular momentum λ. The contribution to the optical potential becomes

$$\Delta U(r)=\sum_{a_1a_2,\lambda}\sqrt{\frac{a_{tr}(a_1,a_2)}{16\pi|\ddot{r}_0|}}(2j_1+1)\times u^2(a_2,I_A)v^2(a_1,I_a)|f_\lambda^{a_2a_1}(r)|^2(-i)\times[g_\lambda(Q)+ip_\lambda(Q)]. \tag{11}$$

Notice that λ in this expansion is the transfer angular momentum. The function f_λ indicates the radial form factor of multipolarity λ, u and v are the occupation numbers of the orbitals involved in the transition and $a_{tr}\approx 1.2$ fm is the decaying length of the radial form factor. The sum has to be extended to all single particle states belonging to the projectile and to the target that can be populated in the reaction. Their contribution is weighted by the quantity $-i[g_\lambda(Q)+ip_\lambda(Q)]$ that corresponds to the integral $I(\omega)$ introduced above, but generalized to account also for the transfer angular momentum λ. Details about this can be found in Refs. [1,3]. Here we would like to point out that in this formalism the contribution from multinucleon transfer channels is included insofar as the transfer proceeds via a successive mechanism. The contribution of pair correlations (transfer of correlated pairs) is not included in the formalism. However pairing correlations are mostly felt by the ground state and nearby levels, and the corresponding transitions are in general hindered by Q-value effects.

In a similar fashion one can evaluate the contribution (11) corresponding to pick-up reaction channels. The potential ΔU is obtained by adding the contribution coming from all the proton and neutron stripping and pick-up reactions.

III. THE CONTINUUM

Close to the drip lines of protons and neutrons the energy of the last occupied orbit may be very close to the continuum threshold. As an illustrative example, we show in Fig. 1 the neutron and proton single particle energies in calcium isotopes. The lightest of these isotopes lies on the proton drip line while the heaviest one is a neutron drip-line nucleus. The displayed single particle energies have being calculated by using the parametrization [4] of the shell model potential, i.e.,

$$V_{sm}(r)=V(r)-\lambda\frac{\lambda_c^2}{2}\frac{1}{r}\frac{dV(r)}{dr}(\vec{s}\cdot\vec{l}) \tag{12}$$

with

$$V(r)=\frac{-V_0}{1+\exp[(r-R)/a]}, \tag{13}$$

where the radius is given by $R=r_0A^{1/3}$, $\lambda_c=\hbar/Mc$ is the reduced Compton wavelength, and M the reduced mass of the nucleons moving around the $(A-1)$ core. The strength of the volume term is given by

$$V_0=49.6\left(1-0.86\frac{N-Z}{N+Z}\right) \tag{14}$$

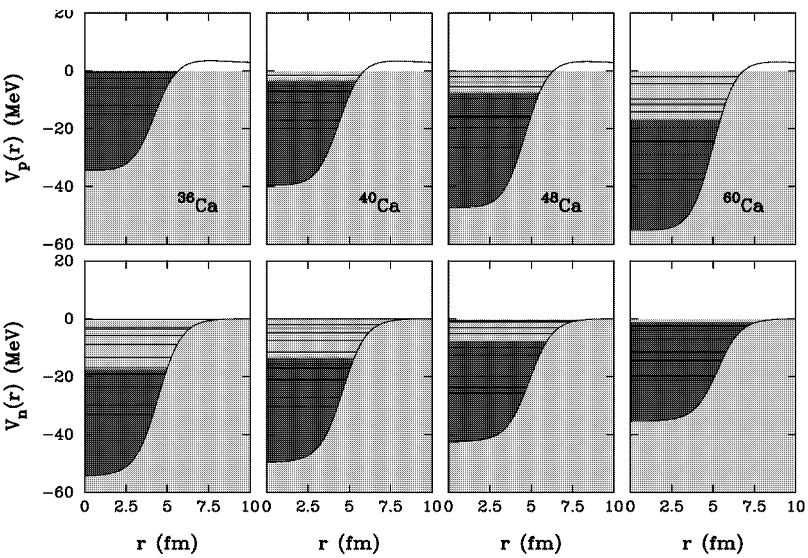

FIG. 1. Neutron (bottom) and proton (top) single particle levels around the Fermi surface for calcium isotopes. The Woods-Saxon potential is also shown. The dark gray region indicates the occupied single-particle orbits, while the light gray indicates the region of bound states.

for neutrons and by

$$V_0=49.6\left(1+0.86\frac{N-Z}{N+Z}\right) \tag{15}$$

for protons. The other parameters are $r_0=1.347$ fm, $r_0^{sl}=1.31$ fm, $a=0.7$ fm, and $\lambda=35$ for neutrons while for protons it is $r_0=1.275$ fm, $r_0^{sl}=1.32$ fm, $a=0.7$ fm, and $\lambda=36$. Of course for protons one has to add the corresponding Coulomb term.

As mentioned above, one can see from Fig. 1 that nuclei on the drip lines are likely to be excited by the transfer reaction onto continuum states. This feature has to be incorporated into the formalism.

The inclusion of the continuum in quantum processes is a very difficult undertaking which has been attacked by using a variety of approaches (see Refs. [5–8]). Within any of these methods the continuum is replaced by a set of discrete states. The form factor corresponding to transitions into the continuum can then be written as

$$f_{a_2a_1}(E_2,\mathbf{r})=\int d^3r_{1A}\phi^{a_2}(E_2,\mathbf{r}_{1A})^*U_{1A}(r_{1A})\phi^{a_1}(\mathbf{r}_{1b}), \tag{16}$$

where $\phi^{a_2}(E_2,\mathbf{r}_{1A})$ is the properly normalized scattering wave function at the bombarding energy E_2 [9].

Expanding the form factor (16) in spherical harmonics one obtains for the contribution to the optical model the expression

$$\begin{aligned}\Delta U_{\mathrm{cont}}(r)=&\sum_{a_1,a_2,\lambda}(2j_1+1)v^2(a_1,I_a)\\&\times\int_0^\infty dE_2\sqrt{\frac{a_{tr}(a_1,a_2)}{16\pi|\ddot{r}_0|}}|f_\lambda^{a_2a_1}(E_2,r)|^2\\&\times(-i)[g_\lambda(Q)+ip_\lambda(Q)].\end{aligned} \tag{17}$$

To obtain this equation we assumed that also in this case the form factor has an exponential decaying behavior. This is indeed the case, as can be seen in Fig. 2 where some representative examples are shown.

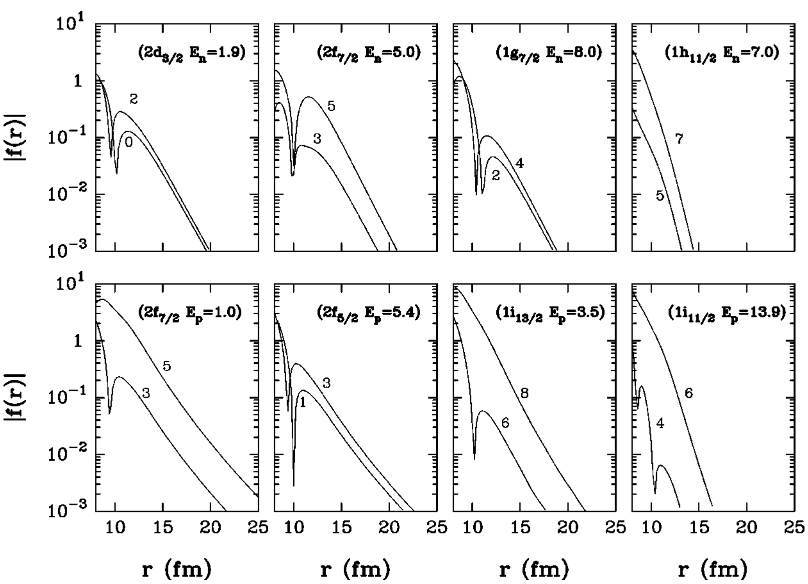

FIG. 2. One-particle transfer form factors involving transitions to the continuum. In the top row are shown the form factors for neutron pick-up reactions corresponding to the transitions from the state $2d_{3/2}$ at -8.5 MeV in ^{124}Sn to the indicated states in the continuum of ^{36}Ca. In the bottom row are shown the form factors for proton stripping corresponding to the transitions from the state $1d_{1/2}$ in ^{36}Ca at -0.5 MeV to the indicated continuum states in ^{124}Sn. The labels of the different curves indicate the corresponding λ transfer.

TABLE I. Resonance states for protons in ^{36}Ca and ^{124}Sn. The label n in the single particle state (nlj) indicates the number of nodes of the wave function in the inner region of the potential.

	^{36}Ca			^{124}Sn	
	E_R (MeV)	Γ (MeV)		E_R (MeV)	Γ (MeV)
$1f_{7/2}$	2.819	0.0025	$2f_{7/2}$	1.1017	5.867×10^{-14}
$2p_{3/2}$	3.827	0.4857	$1i_{13/2}$	3.4836	2.314×10^{-8}
$2p_{1/2}$	5.089	1.5544	$3p_{3/2}$	3.4999	8.870×10^{-4}
$2d_{5/2}$	7.709	4.9022	$1h_{9/2}$	3.6083	1.717×10^{-7}
$1f_{5/2}$	9.894	1.1741	$3f_{5/2}$	5.4078	4.571×10^{-2}

The implementation of Eq. (17) is very demanding if there are narrow resonances, as indeed often occurs in shell model potentials. In such a case it becomes difficult to know *a priori* the step ΔE_2 to perform the energy integral, since at the position of the resonance the scattering wave function increases enormously in a very small energy interval.

The presence of narrow resonances is a common property of shell model potentials both for stable and drip-lines nuclei. As an example we show in Table I resonances corresponding to different (l,j) values that we evaluated for the nuclei ^{36}Ca and ^{124}Sn using the code ESTAR [10]. For some of these resonances the width is very small and to perform the integration over the energy within a reasonable accuracy one has to use such a small step of integration that the calculation becomes too lengthy. It is thus important to find another strategy to carry out that integration.

In order to analyze this problem we first study the dependence of the total cross section to populate states in the continuum as a function of their energy (which we call E_2). This is easily done in first order perturbation theory by applying the formalism presented above. Here we only recall that the cross section is proportional to the integral of the form factor along the classical trajectory modulus square. As an example we consider a proton stripping reaction in the collision of ^{20}Ne on ^{208}Pb at a bombarding energy close to the Coulomb barrier. Using the Woods-Saxon parameter of Ref. [4] we found in ^{208}Pb a narrow proton resonance corresponding to the state $j_{15/2}$ at an energy of 3.866 MeV and a width of 0.001 MeV. We then calculated the total cross section to

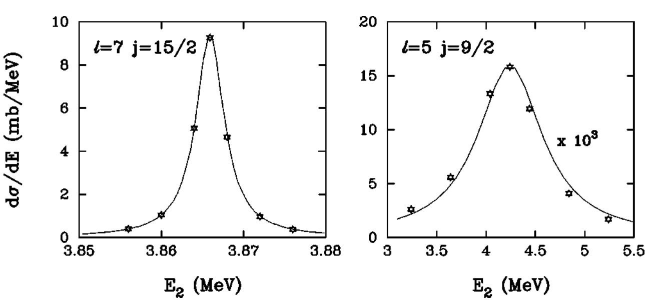

FIG. 3. Total cross section as a function of the energy corresponding to the transfer of a proton in ^{20}Ne to the state (l,j) lying in the continuum part of the spectrum of ^{208}Pb. The values of (l,j) are indicated in the figure. For the state with the larger width (right part) the cross section has been multiplied by a factor 10^3. The full line is a Breit-Wigner distribution with parameters corresponding to the complex energy of the resonance (l,j). The stars are the calculated values.

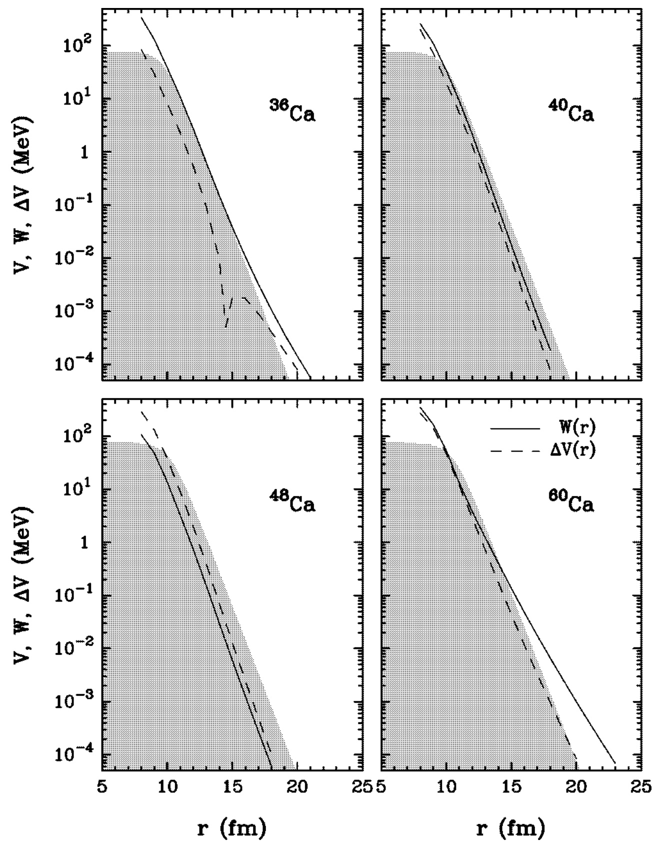

FIG. 4. Absorption (full line) and polarization potential (dash line) for the reaction of the indicated Calcium isotopes on ^{124}Sn. The shaded area is the real potential. Notice that for ^{36}Ca the polarization potential becomes repulsive at large distances.

populate this state by varying the energy E_2 around the value 3.866 MeV. The resulting cross section as a function of E_2 is shown on the left hand side of Fig. 3. The stars on this figure indicate the calculated values while the continuous line is a Breit-Wigner distribution corresponding to the energy and width of the resonance.

We performed the same calculation for the resonance $h_{9/2}$, which is much wider than the previous one. The results are shown on the right-hand side of Fig. 3. Even in this case the energy dependence of the cross section is well described by a Breit-Wigner distribution with parameters corresponding to the complex energy of the resonance.

From these plots one sees that for a given resonance $a \equiv (lj)$ the cross section can be parametrized according to the expression

$$\sigma(E_2)=\frac{\Gamma_a^2}{4(E_2-E_a)^2+\Gamma_a^2}\,\sigma(E_a), \tag{18}$$

where we have indicated with E_a the real part of the energy of the resonance, Γ_a its width and $\sigma(E_a)$ is the value of the cross section at the resonance. This is an important feature since it will allow us to evaluate the imaginary and polarization potentials considering only bound states and resonances, without performing the energy integral. Indeed, by defining the form factor of a resonance as

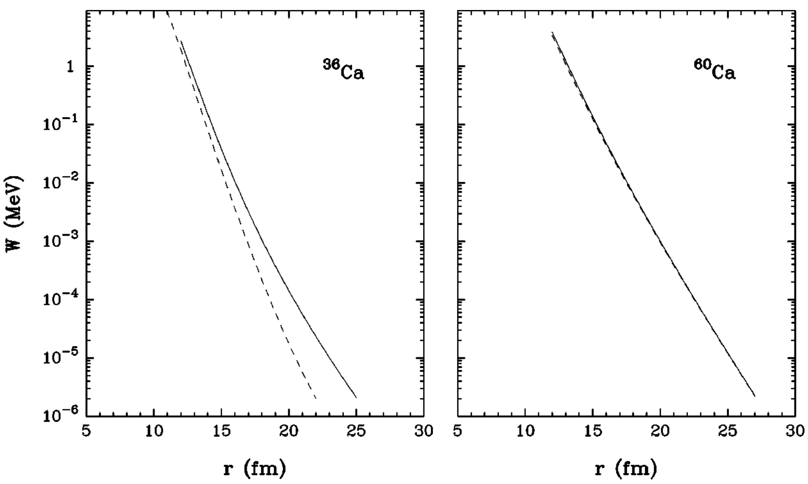

FIG. 5. Total absorption (full line) and the corresponding contribution from bound states only (dash line) for the reaction on ^{124}Sn.

$$f_{a_1a_2}(E_a,r)=\sqrt{\frac{\pi\Gamma_a}{2}}f_{a_1a_2}(E_a,r), \tag{19}$$

where the factor $\pi\Gamma_a/2$ is the integral of the Breit-Wigner distribution in Eq. (18) over the energy, we can calculate the polarization potential by using Eq. (11) but now the sum has to be extended also to the resonance states.

IV. RESULTS AND CONCLUSIONS

Since in drip-line nuclei excitations to states in the continuum can readily occur, one may expect that in these nuclei the parametrization of the optical potential does not follow standard prescriptions, i.e., those that have been derived for stable nuclei [13]. In this section we will examine this question in detail. For this we will consider reactions involving stable as well as proton and neutron drip-line nuclei. We will thus apply Eq. (11) and Eqs. (17)–(19) to study the correction to the optical potential for the collision of stable and drip-line calcium isotopes on ^{124}Sn. To have a meaningful comparison in all cases we set the center of mass bombarding energy to be 10% over the nominal Coulomb barrier. The choice of these reactions has been dictated by the fact that for the stable calcium isotopes there exist experiments [11,12] that have been analyzed within a generalization of the semiclassical model used in this paper.

Including all the neutron and proton bound states in the projectile as well as in the target and all the resonances with energies below 20 MeV we have calculated the imaginary and polarization potentials for the reactions mentioned above. The calculated imaginary part of the potential (full line) is shown in Fig. 4 in comparison with the real part of the empirical optical potential (shaded area) taken from Ref. [13].

An important feature to be noticed in this figure is that for drip-line nuclei the imaginary part of the potential is at least as large as the corresponding real part. In stable nuclei, instead, the real part is larger than the imaginary one by a factor of about 5. This indicates that in drip-line nuclei the scattering is dominated by absorption and, therefore, one may need to use coupled channels techniques to analyze grazing reactions in those nuclei.

It is also worthwhile to notice that in the case of ^{36}Ca the polarization potential (dotted line) has at large distances a node and therefore beyond that point this potential reduces the attractive part of the optical potential. But this effect, which as seen in the figure is small, may strongly depend upon the parameters of the shell model potential that define the position of the single particle bound and resonance states. This feature usually does not appear in stable nuclei, neither in the other calcium isotopes of the figure. That is, only in ^{36}Ca the shape of the bare nucleus-nucleus interaction may be affected by the polarization.

As was pointed out above, the influence of the continuum should be relevant only for nuclei close to the drip line, since in stable nuclei the contribution of the continuum is strongly suppressed by the adiabatic cutoff function $g_\lambda(Q)+ip_\lambda(Q)$ in Eq. (11). This feature indeed appears in our calculations and, therefore, we will only present drip-line nuclei. Thus, in Fig. 5 a comparison between the imaginary potentials calcu-

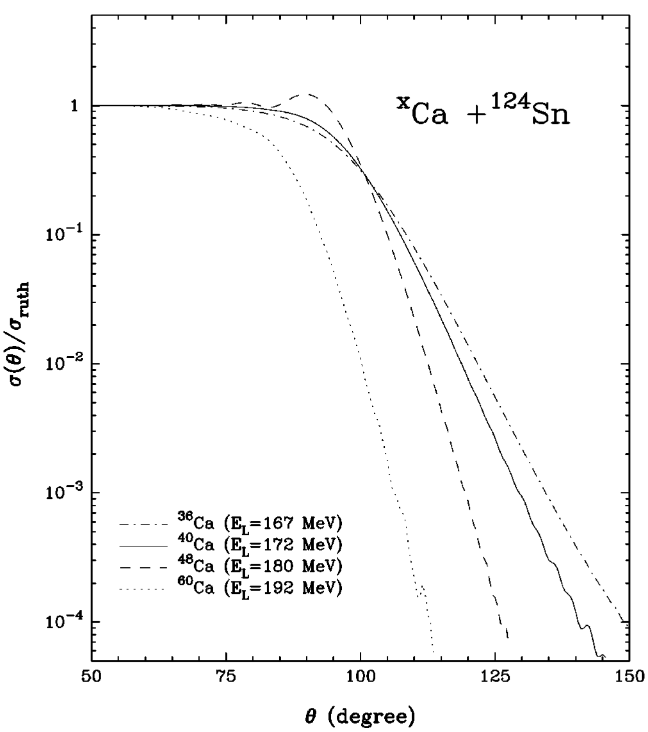

FIG. 6. Elastic angular distribution (ratio to Rutherford) for the collision of calcium isotopes on ^{124}Sn at the indicated bombarding energy.

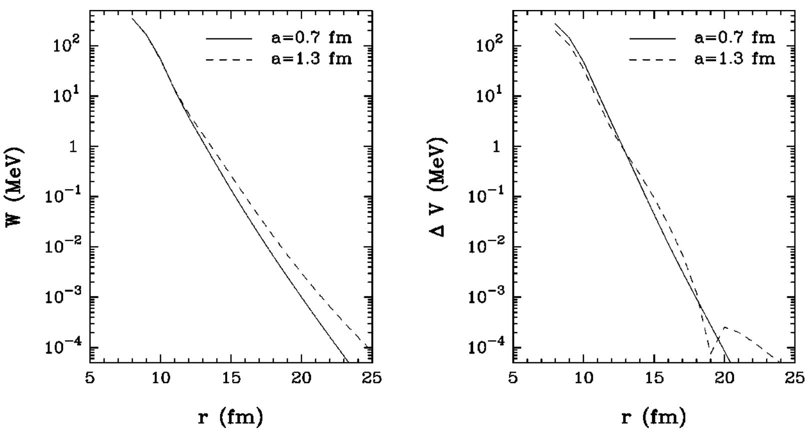

FIG. 7. Total absorption W and polarization ΔV potentials for the case of ^{60}Ca corresponding to different values of the diffusivity of the shell model potential as discussed in the text.

lated by including only bound states (dashed line) and bound states plus the resonances (full line) is presented for ^{36}Ca and ^{60}Ca. As one can see, at this low bombarding energy, only for the proton drip-line nuclei the continuum plays a role while it is unimportant in all the other cases. In ^{36}Ca the continuum actually is very important at large distances, but this region does not influence the shape of the elastic angular distribution.

In Fig. 6 we show the elastic angular distribution provided by these potentials. One sees that the relatively strong imaginary part of the potential corresponding to ^{36}Ca and ^{60}Ca, as discussed above, is reflected in the modifications of the cross section at forward angles.

Finally, one may expect that in nuclei close to the neutron drip line the corresponding density presents a long tail forming a ''neutron skin.'' This feature was analyzed in some detail in Ref. [14] within the framework of a mean field approach. It was found there that going from stable nuclei to the ones on the neutron drip line there is a variation in the diffusivity a by a factor of as much as 2. At the same time the depth V_0 of the potential diminishes by $\approx 10\%$. To see the effect of these changes on our potentials, we repeated our calculation for the nucleus ^{60}Ca by using $a = 1.3$ fm and decreasing V_0 by 10%. As seen in Fig. 7 the corresponding changes in the absorption and polarization potentials are not very important. The corresponding elastic cross sections are not affected.

In conclusion, in this paper we have generalized the formalism of Refs. [1,3] to incorporate the contribution of the continuum. This allows us to calculate the absorptive and polarization potentials even for system at the limit of the β-stability valley. For collisions with nuclei close to the neutron and proton drip lines the optical potential is dominated by the absorption and the polarization potential may be repulsive. This finding may indicate that for exotic nuclei coupled-channel calculations may be needed even to describe transfer processes.

ACKNOWLEDGMENT

This work has been supported by the Göran Gustaffson Foundation.

[1] R.A. Broglia, G. Pollarolo, and A. Winther, Nucl. Phys. **A361**, 301 (1981).
[2] G. Pollarolo, R.A. Broglia, and A. Winther, Nucl. Phys. **A406**, 369 (1983).
[3] C.H. Dasso, S. Landowne, G. Pollarolo, and A. Winther, Nucl. Phys. **A459**, 134 (1986).
[4] S. Cwiok, J. Dudek, W. Nazarewicz, J. Skalski, and T. Werner, Comput. Phys. Commun. **46**, 379 (1987).
[5] T. Berggren, Nucl. Phys. **A109**, 265 (1968).
[6] C. Mahaux and H. A. Weidenmüller, *Shell Model Approach to Nuclear Reactions* (North-Holland, Amsterdam, 1969).
[7] A. Bonaccorso and D. N. Brink, Phys. Rev. C **44**, 1559 (1991).
[8] R. J. Liotta, E. Maglione, N. Sandulescu, and T. Vertse, Phys. Lett. B **367**, 1 (1996).
[9] R. G. Newton, *Scattering Theory of Waves and Particles* (Springer-Verlag, New York, 1982), p. 180.
[10] E. Maglione, Computer code ESTAR (unpublished).
[11] L. Corradi, J.H. He, D. Ackermann, A.M. Stefanini, A. Pisent, S. Beghini, G. Montagnoli, F. Scarlassara, G.F. Segato, G. Pollarolo, C.H. Dasso, and A. Winther, Phys. Rev. C **54**, 201 (1996).
[12] L. Corradi, A.M. Stefanini, J.H. He, S. Beghini, G. Montagnoli, F. Scarlassara, G.F. Segato, G. Pollarolo, and C.H. Dasso, Phys. Rev. C **56**, 938 (1997).
[13] Ö. Akyüz and A. Winther, in *Prooceedings of Enrico Fermi International School of Physics 1979*, edited by R.A. Broglia, C.H. Dasso, and R. Ricci (North Holland, Amsterdam, 1981).
[14] J. Dobaczewski, W. Nazarewicz, T.R. Werner, J.F. Berger, C.R. Chinn, and J. Dechargé, Phys. Rev. C **53**, 2809 (1996).